UCLA
COMPUTATIONAL AND APPLIED MATHEMATICS

Capturing Shock Reflections: An Improved Flux Formula

Rosa Donat
Antonio Marquina

April 1995

CAM Report 95-19

Department of Mathematics
University of California, Los Angeles
Los Angeles, CA. 90024-1555

Capturing Shock Reflections: An improved flux formula

Rosa Donat* Antonio Marquina*

April 16, 1995

Abstract

Godunov type schemes, based on exact or approximate solutions to the Riemann problem, have proven to be an excellent tool to compute approximate solutions to hyperbolic systems of conservation laws. However, there are many instances in which a particular scheme produces inappropriate results. In this paper we consider several situations in which Roe's scheme gives incorrect results (or blows up all together) and propose an alternative flux formula which produces more accurate numerical approximations.

Key Words. Nonlinear Systems of Conservation Laws, Shock Capturing schemes, Shock Reflections.

AMS-MOS Classification: Primary 65M05, Secondary 65M10

1 Introduction

Shock capturing techniques for the computation of discontinuous solutions to hyperbolic conservation laws are based on an old (by now) theorem of Lax and Wendroff establishing that the limit solutions of a consistent scheme in conservation form are in fact weak solutions to the PDE and, thus, their discontinuities will propagate at the right speeds.

Over the years, it has become clear that one of the most successful strategies for designing a shock capturing scheme is to follow Godunov's lead and use the solution to the Riemann problem (the only initial-value problem easy enough to be solved explicitly) as an essential building block of the scheme.

*Departamento de Matemática Aplicada Universitat de València 46100-Burjassot (València) SPAIN Supported by DGICYT PS90-0265, in part by a Grant from the I.V.E.I., in part by a Grant from Universitat de València and computer time supported in part by ARPA URI Grant ONR-N00014-92-J-1890

Godunov assumed that a flow solution could be represented by a series of piecewise constant states with discontinuities at the cell interfaces. A piecewise constant function is a reasonable numerical representation of the solution in regions of smooth flow and it is specially well suited near discontinuities. The discretized flow solution is evolved by considering the nonlinear interaction between its component states. Viewed in isolation, each pair of neighboring states constitutes a Riemann problem, which can be solved exactly. If there is no interaction between neighboring Riemann problems, the global solution is easily found by piecing together these Riemann solutions. The approximate solution at the next time level is then obtained averaging over each cell this global solution.

The method can be written in conservation form since it uses solutions to Riemann problems which are themselves exact solutions of the conservation laws and, because it mimics much of the relevant physics, Godunov's scheme results in an accurate and well-behaved treatment of shock waves.

For Gas Dynamics simulations, Godunov's method computes the exact solution to a Riemann problem at each cell interface. However, most of the structure of the exact solution is lost in the averaging process used to update each cell value. This observation suggests that it may not be worthwhile calculating the Riemann solution exactly. In fact, one may be able to obtain equally good numerical results with an approximate Riemann solution obtained by some less expensive means.

Roe's scheme is based on a local linearization that makes the solution of the Riemann problem a trivial task. The solution to Roe's linearized Riemann problem coincides with the solution to the exact problem whenever this involves merely a single shock or contact discontinuity. On the other hand since rarefaction waves do not appear in linear systems, the scheme can (and does) produce non-physical expansion shocks in the computed flows.

Other approximate Riemann solvers, based on Roe's simplification, have emerged over the years. Their basic design principle is (as in Roe's scheme) that it might be sufficient to find only an approximate solution to a Riemann problem, provided that this approximate solution still describes important nonlinear behavior ([9, 3]).

Godunov type schemes are indeed very robust in most situations. However, they can, on occasions, fail quite spectacularly. For example when computing shock reflection problems in one dimension, most shock capturing schemes produce an unphysical 'overheating' near the reflecting wall [13]. In two dimensions, Roe's method can sometimes admit solutions with an inexplicably kinked Mach stem.

Reports on approximate Riemann solver failures and their respective corrections are abundant in the literature (see e.g. [15] and references therein). It should be noted that the failures of a specific Riemann solver may usually be repaired by the judicious use of a small amount of artificial dissipation. However, this technique often implies the tuning and re-tuning of various parameters,

which degrades the automatic character of Godunov type schemes. Moreover, the type and amount of viscosity to be added in each particular deficiency is, usually, not the same, further aggravating the user.

A different strategy, described by Quirk [15], is to combine two or more solvers. With this approach, it is possible to control certain instabilities by changing the flavour of the dissipation mechanism rather than increasing the absolute level of dissipation.

Quirk's approach is very attractive, although still has a user-problem dependent parameter left: when and where to use one Riemann solver in preference to another.

Our approach is similar to that of Quirk's. We do combine Roe's solver with a Lax Friedrichs type of scheme to produce an entropy satisfying, shock capturing scheme, but the two solvers are intertwined in a more intrinsic way so that there are no adjustable parameters in the scheme.

In the present paper we address various instances in which there is a recognized failure of Roe's solver and propose an improved flux formula that seems to alleviate or cure the problem.

The paper is organized as follows: In section 2 we describe Marquina's flux formula for systems of hyperbolic conservation laws. In the scalar case, it corresponds to a flux formula used by Shu and Osher [20]. In Section 3 we apply it to Burger's equation and compare the numerical results with those obtained with the flux-splitting scheme of Steger and Warming. Section 4 is devoted to the analysis of the overheating phenomenon that appears in shock reflection experiments, and to several somewhat related questions. In Section 5, Marquina's scheme is used to approximate a slowly moving shock wave. We measure the level of noise generated by the scheme in the downstream region of the shock wave and compare it to that of Roe's scheme. Section 6 shows the performance of the proposed flux formula in 2D flows, analyzing the classical Mach 3 step flow. Some conclusions are drawn in Section 7.

2 Roe's Flux formula, Flux-splitting schemes and an improved flux formula

Disregarding entropy considerations, Roe's solver applied to a system of conservation laws in one dimension

$$\mathbf{u}_t + (\mathbf{f}(\mathbf{u}))_x = 0 \tag{1}$$

yields a conservative method whose numerical flux function is computed as follows:

$$\mathbf{F}^R(\mathbf{u}_l, \mathbf{u}_r) = \frac{1}{2}\left(\mathbf{f}(\mathbf{u}_l) + \mathbf{f}(\mathbf{u}_r) - \sum_p |\lambda_p|\alpha_p \mathbf{r}^p\right) \tag{2}$$

where

$$\alpha_p = \mathbf{l}^p \cdot (\mathbf{u}_l - \mathbf{u}_r)$$

and λ_p, $\mathbf{r}^p$ and $\mathbf{l}^p$ are the eigenvalues, right and left eigenvectors respectively of $\tilde{A} = A(\tilde{\mathbf{u}}) = A(\mathbf{u}_l, \mathbf{u}_r)$, the Jacobian matrix $(\partial \mathbf{f}(\mathbf{u})/\partial \mathbf{u})$ at $\tilde{\mathbf{u}}$, the 'Roe mean' of the left and right states (see e.g. [10]).

Van Leer [23] considers the upwind-differencing first order schemes of Godunov and Roe for the inviscid Burgers equation and observes that the difference between these two schemes lies only in the treatment of a transonic expansion. Where the exact Riemann solution, used in Godunov's method, would include an expansion fan, Roe's method puts in a so called expansion shock.

The inability of Roe's solver to account for rarefaction waves leads to entropy violating discontinuities. To prevent these expansion shocks, one has to modify the flux function in Roe's scheme. Harten and Hyman [7] introduce an intermediate state that simulates the diffusion introduced to a Godunov-type scheme by a continuous transition between the left and right states. Roe [18] describes another modification that breaks down expansion shocks and it also eliminates the 'glitches' (dogleg phenomenon) that appear in most first order schemes.

In the scalar case, Marquina's flux formula is a combination of Roe's flux and a Local-Lax-Friedrichs (LLF from now on) flux utilized by Shu and Osher in [20] and labeled F^{RF} :

$$F^{RF}(u_l, u_r) = \begin{cases} f(u_l) & \text{if} \quad f' > 0 \ \text{ in } \ [u_l, u_r] \\ f(u_r) & \text{if} \quad f' < 0 \ \text{ in } \ [u_l, u_r] \\ \frac{1}{2}(f(u_l) + f(u_r) - \alpha(u_r - u_l)) & \text{else} \end{cases} \tag{3}$$

$$\alpha = \max_{u \in [u_l, u_r]} |f'(u)| \tag{4}$$

In this section, $[u_l, u_r]$ should be understood as the range of u-values that lie between u_l and u_r.

For a convex conservation law, Roe's scheme is equivalent to Godunov's except at transonic rarefactions. Thus, we use Roe's scheme except when we suspect the occurrence of a transonic rarefaction, in which case we switch to the more viscous, entropy satisfying Lax-Friedrichs scheme.

It can be verified (see [20]) that the LLF flux

$$F^{LLF}(u_l, u_r) = \frac{1}{2}\left(f(u_l) + f(u_r) - \alpha(u_r - u_l)\right)$$

is monotone, hence F^{RF} is an 'entropy fix' for Roe's flux.

In the convex case, we only need to switch to LLF when $f'(u_l) < 0 < f'(u_r)$ but the experiments reported in [20] and our own experimentation confirms that conservative schemes whose numerical flux function is F^{RF} always approximates the physically relevant solution even for non convex f. Moreover, local pathologies, like the dogleg effect, either do not show up in numerical approximations,

or are reduced to $O(\Delta x)$ glitches in the first order version of the scheme. Higher order versions completely eliminate the pathology.

The extension to systems of conservation laws differs from that of [20] and follows two basic directions. On one hand, Roe's linearization (or any linearization, as pointed out in [4]) may not always be appropriate, specially when dealing with systems of conservation laws other than the Euler equations for which the 'Roe mean' might not be easily computed (or even known). Along this line, and still in the upstream-differencing spirit, we shall make use of two sets of eigenvalues and eigenvectors, one coming from the left state and the other coming from the right state, to compute the flux at a given interface.

On the other hand, the combination of Roe's solver with the LLF scheme is done *locally*. The choice of scheme is done in each 'local' characteristic field, thus the scheme for systems of conservation laws mimics the properties of the scheme for the scalar conservation law.

The algorithmic description of Marquina's improved flux formula is as follows:

Given the left and right states, we compute the *'sided'* local characteristic variables and fluxes:

$$\begin{array}{rclcrcl} \omega_l^p & = & \mathbf{l}^p(\mathbf{u}_l)\cdot\mathbf{u}_l & \qquad & \phi_l^p & = & \mathbf{l}^p(\mathbf{u}_l)\cdot\mathbf{f}(\mathbf{u}_l) \\ \omega_r^p & = & \mathbf{l}^p(\mathbf{u}_r)\cdot\mathbf{u}_r & & \phi_r^p & = & \mathbf{l}^p(\mathbf{u}_r)\cdot\mathbf{f}(\mathbf{u}_r) \end{array}$$

for $p = 1, 2 \ldots, m$. Here $\mathbf{l}^p(\mathbf{u}_l)$, $\mathbf{l}^p(\mathbf{u}_r)$, are the left eigenvectors of the Jacobian matrices $A(\mathbf{u}_l)$,$A(\mathbf{u}_r)$.

Let $\lambda_1(\mathbf{u}_l), \ldots, \lambda_m(\mathbf{u}_l)$ and $\lambda_1(\mathbf{u}_r), \ldots, \lambda_m(\mathbf{u}_r)$ be their corresponding eigenvalues. We proceed as follows:

For $k = 1, \ldots, m$

If $\lambda_k(\mathbf{u})$ does not change sign in $[\mathbf{u}_l, \mathbf{u}_r]$,then

If $\lambda_k(\mathbf{u}_l) > 0$ then
$\phi_+^k = \phi_l^k$
$\phi_-^k = 0$
else
$\phi_+^k = 0$
$\phi_-^k = \phi_r^k$
endif

else

$$\alpha_k = \max_{\mathbf{u}\in\Gamma(\mathbf{u}_l,\mathbf{u}_r)} |\lambda_k(\mathbf{u})|$$

$\phi_+^k = .5(\phi_l^k + \alpha_k\omega_l^k)$
$\phi_-^k = .5(\phi_r^k - \alpha_k\omega_r^k)$

endif

$\Gamma(\mathbf{u}_l, \mathbf{u}_r)$ is a curve in phase space connecting $\mathbf{u}_l$ and $\mathbf{u}_r$. For the Euler equations of gas dynamics, the fields are either genuinely nonlinear or linearly degenerate, hence we can test the possible sign changes of $\lambda_k(\mathbf{u})$ by checking the sign of $\lambda_k(\mathbf{u}_l) \cdot \lambda_k(\mathbf{u}_r)$. Also, α_k can be determined as

$$\alpha_k = \max\{|\lambda_k(\mathbf{u}_l)|, |\lambda_k(\mathbf{u}_r)|\}.$$

Marquina's flux formula is then:

$$\mathbf{F}^M(\mathbf{u}_l, \mathbf{u}_r) = \sum_{p=1}^{m} \left(\phi_+^p \mathbf{r}^p(\mathbf{u}_l) + \phi_-^p \mathbf{r}^p(\mathbf{u}_r)\right) \tag{5}$$

where $\mathbf{r}^p(\mathbf{u}_l)$, $\mathbf{r}^p(\mathbf{u}_r)$, are the right eigenvectors of the Jacobian matrices $A(\mathbf{u}_l)$,$A(\mathbf{u}_r)$.

The first order scheme is thus,

$$\mathbf{u}_j^{n+1} = \mathbf{u}_j^n + \frac{\Delta x}{\Delta t}(\mathbf{F}^M(\mathbf{u}_j^n, \mathbf{u}_{j+1}^n) - \mathbf{F}^M(\mathbf{u}_{j-1}^n, \mathbf{u}_j^n))$$

Marquina's numerical flux is consistent, i.e.

$$\mathbf{F}^M(\mathbf{u}, \mathbf{u}) = \mathbf{f}(\mathbf{u}),$$

and it is easy to see that, when applied to a constant coefficient scalar system, Marquina's scheme is equivalent to Roe's and would yield the exact solution to the Riemann problem.

Notice also that when all signal speeds associated to the numerical flux $\mathbf{F}^M(\mathbf{u}, \mathbf{v})$ are > 0 then

$$\mathbf{F}^M(\mathbf{u}, \mathbf{v}) = \mathbf{f}(\mathbf{u})$$

and when all signal speeds are < 0,

$$\mathbf{F}^M(\mathbf{u}, \mathbf{v}) = \mathbf{f}(\mathbf{v}).$$

Marquina's numerical flux (5) resembles a flux-splitting formula, with

$$\mathbf{F}^M(\mathbf{u}, \mathbf{v}) = \mathbf{F}^+(\mathbf{u}) + \mathbf{F}^-(\mathbf{v})$$

where

$$\mathbf{F}^+(\mathbf{u}) = \sum \phi_+^p \mathbf{r}^p(\mathbf{u}), \qquad \mathbf{F}^-(\mathbf{u}) = \sum \phi_-^p \mathbf{r}^p(\mathbf{u}) \tag{6}$$

but the characteristic numerical fluxes $\phi_\pm = \phi_\pm(\mathbf{u}, \mathbf{v})$, i.e. they depend (in a nonlinear way) on the left and right states. Formulas (6) are, in fact, a bit misleading. Technically, (5) is not a flux splitting formula as described in [9].

Higher accuracy is obtained by a nonlinear interpolation procedure of either the fluxes [20] or the dependent variables [10, 1] and a Runge-Kutta time stepping procedure [20].

There are a variety of reconstruction procedures available to increase the formal order of spatial accuracy of the method. In our experiments, we have chosen

the ENO (Essentially Non Oscillatory) polynomials of Harten et al. [10], Van Leer's piecewise linear reconstruction [22], and Marquina's piecewise hyperbolic method (PHM) [11].

ENO techniques (including the PHM) use a local adaptive stencil to obtain information automatically from regions of smoothness when the solution develops discontinuities. As a result, approximations using these methods can obtain uniformly high-order accuracy right up to the discontinuities, while keeping a sharp, essentially non-oscillatory shock transition (see [11, 10] and references therein).

If $\mathbf{R}(\cdot, \mathbf{u}^n)$ is a reconstruction procedure that computes an $O(h^p)$ approximation to $\mathbf{u}(x, t_n)$ from the cell values $\{\mathbf{u}^n\}$, then the p^{th} order version of the scheme based on such reconstruction procedure is obtained following a semi-discrete formulation, i.e.

$$\frac{d}{dt}\mathbf{u}_j(t) = -\frac{1}{\Delta x}[\tilde{\mathbf{f}}_{j+1/2} - \tilde{\mathbf{f}}_{j-1/2}] \tag{7}$$

where

$$\tilde{\mathbf{f}}_{j+1/2} = \mathbf{F}\left(\mathbf{R}(x_{j+1/2} - 0; \mathbf{u}(t)), \mathbf{R}(x_{j+1/2} + 0; \mathbf{u}(t))\right)$$

and $\mathbf{F}(\mathbf{u}_1, \mathbf{u}_2)$ is the exact or approximate Riemann solver flux to be used.

Considering (7) to be a system of ordinary differential equations in t for the vector $\mathbf{u}(t) = \{\mathbf{u}_j(t)\}$, we solve the problem using a numerical ODE solver. In particular, in our experiments we use Shu and Osher [20] TVD Runge-Kutta solvers of second and third order.

We recall (see [10, 11]) that these scalar reconstructions are non-oscillatory only if the discontinuities are separated by at least $r + 1$ points of smoothness, where r is the order of accuracy of the reconstruction. Consequently, a component-by-component reconstruction procedure may cease to be non-oscillatory around the discrete set of points where discontinuities of the solution interact, and can produce 'noise' around this set of points. One can largely avoid the noise derived from this fact by applying the reconstruction procedure to the "local characteristic variables" (see [10]).

In [20], Shu and Osher use the moving-stencil idea directly on numerical fluxes to get ENO schemes without using cell-averages. For systems the reconstruction procedure is applied in each 'local characteristic field', and the starting point in the choice of stencil process has to be done in an 'upwind' way. We refer to [20] for further details.

We have implemented the higher order versions of the method following both approaches obtaining very similar results.

3 The scalar conservation law

For illustrative purposes, we include an experiment with Burgers' equation to compare Marquina's solver, Roe's solver and the flux-splitting scheme of Steger

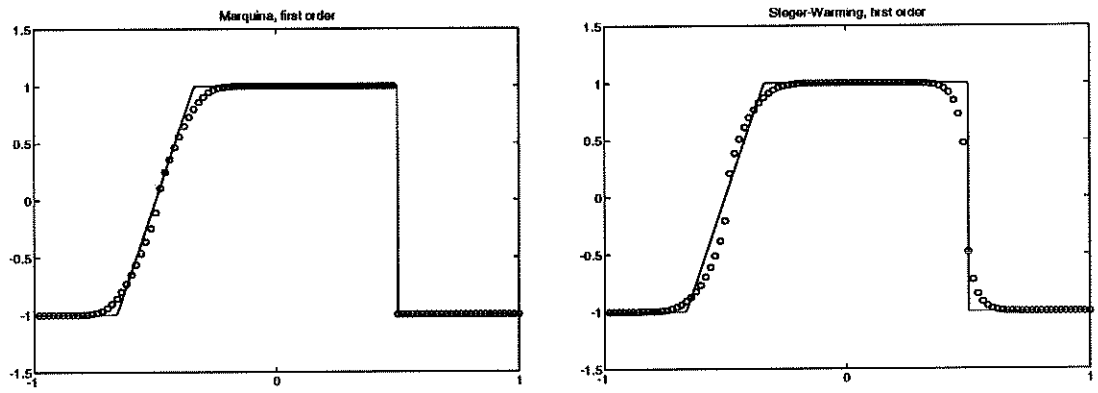

Figure 1: First Order Schemes

and Warming [21].

Steger and Warming's flux function for the scalar conservation law

$$u_t + (f(u))_x = 0$$

is as follows:

$$F^{SW}(u_l, u_r) = \frac{1}{2}\left(f(u_l) + f(u_r) - (|f'(u_r)| \cdot u_r - |f'(u_l)| \cdot u_l)\right)$$

Its lack of smoothness at sonic points has been reported by various authors [9, 24].

Let us consider the following IVP:

$$\begin{aligned} u_t + (\tfrac{u^2}{2})_x &= 0 \\ u(x,0) &= \begin{cases} -1 & \text{if } x < -.5 \\ 1 & \text{if } -.5 < x < .5 \\ -1 & \text{if } x > .5 \end{cases} \end{aligned} \tag{8}$$

Its solution consists of a centered rarefaction wave that contains a sonic point at $x = -0.5$ and a shock wave moving to the right. Figure 1 shows the approximate solutions obtained with first order schemes based on F^{RF} (which is the scalar version of Marquina's flux formula) and F^{SW}. Roe's scheme (not shown) substitutes the rarefaction wave by an unphysical expansion shock.

Notice that the shock transition in the numerical approximation obtained with F^{RF} is as good as Roe's (which is consistent with its design principle) The rarefaction wave is well represented, although we observe an $O(\Delta x)$ glitch at the sonic point This is to be expected, since only the sonic flux (the flux at the interface across which the characteristic speed changes sign) is modified (see Roe [18]).

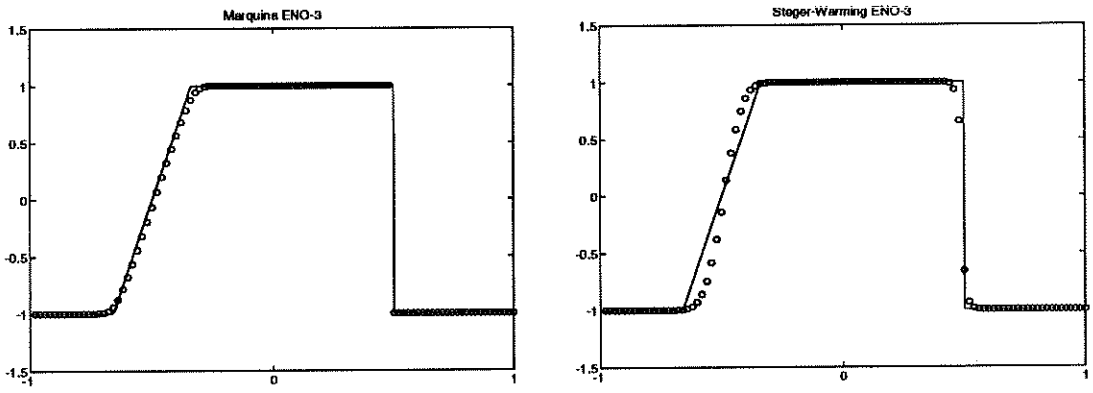

Figure 2: Third Order Schemes

On the other hand, the lack of smoothness of F^{SW} at the sonic point results in a much larger glitch. Also, the smearing of the shock is considerably larger.

Figure 2 shows a third order version of both schemes. The sonic region is now very smooth and accurate when using F^{RF}, while Steger and Warming's formulation produces rarefaction wave which is much too steep.

In all figures, the solid line is the true solution.

4 Shock Reflections, overheating and related matters

We study now the problem of a strong shock reflecting from a rigid wall. Conventional schemes applied to this problem give numerical approximations with a consistent $O(1)$ error in the density and internal energy next to the wall.

W.F. Noh [13] investigated the "excess heating error" in the context of the artificial viscosity approach. Noh defines this error as the excess wall (or piston) heating, due to the artificial viscosity terms which occurs on shock formation (e.g. at a rigid wall where a gas is brought to rest and a shock propagated away, or at the sudden start up of a piston).

This type of error occurs in the first few zones near the wall and shows up as a peak in the specific internal energy (overheating) or, equivalently, a dip in the density. His analysis and experimentation leads him to conclude that the error is inevitable because it is built into the exact solution to the differential equations defining the artificial viscosity method. In fact he goes one step further and argues that such an error will necessarily occur for any shock-smearing method (in the absence of heat conduction) whether the viscosity occurs explicitly in the method or not.

In real fluids, heat conduction is present and this excess wall heating would

not occur (since any hot spot would be quickly dissipated). Thus, Noh concludes that any method which introduces a heat conducting mechanism will, in principle, be able to reduce or even eliminate the overheating. Noh gives one such method in the artificial viscosity context.

Similar conclusions are attained by Menikoff in [12], where a detailed analysis of the wall heating error (again for artificial viscosity methods in Lagrangian and Eulerian formulations) is performed. Menikoff's arguments also lead him to conjecture that all shock capturing schemes without significant heat conduction will have the same type of qualitative entropy error.

Problems of this type have also been investigated by Glaister for more general equations of state [6]. The same phenomenon can be observed in his experiments.

Let us consider the one dimensional Euler equations of gas dynamics for a polytropic gas, i.e. (1) with

$$\mathbf{u} = (\rho, M, E)^T, \qquad \mathbf{f}(\mathbf{u}) = q\mathbf{u} + (0, P, qP) \tag{9}$$

where ρ,q,M,E and P are the density, velocity, moment, energy and pressure respectively, with the following initial conditions at $t = 0$.

$$(\rho(x), q(x), P(x)) = (\rho_0, q_0, P_0), \quad 0 < x < 1 \tag{10}$$

This represents a gas of constant density and pressure moving towards $x = 1$ (provided $q_0 > 0$). The boundary at $x = 1$ is a rigid wall and the exact solution describes the shock reflection from the wall. The gas is brought to rest at $x = 1$ and, denoting the pre-shock values by $(-)$ and the post-shock values by $(+)$ we can postulate an exact solution of the form

$$\rho = \rho^+ \qquad q = q^+ = 0 \qquad P = P^+ \qquad \text{for } x/t > S$$

$$\rho = \rho^- = \rho_0 \qquad q = q^- = q_0 \qquad P = P^- = P_0 \qquad \text{for } x/t < S$$

where S is the speed at which the shock moves out of the wall, given by the Rankine-Hugoniot jump relations, i.e.

$$S = \frac{[\rho u]}{[\rho]} = \frac{[P + \rho u^2]}{[\rho u]} = \frac{[u(e + P)]}{[e]}.$$

In our numerical experiments we take

$$P_0 = 10^{-3}; \qquad \rho_0 = 1; \qquad q_0 = 1$$

and the ideal gas equation of state with $\gamma = 5/3$. Our results with Roe and Marquina's schemes are shown in figures 3 and 4. Here, $\Delta t/\Delta x = 0.2$

Figure 4 shows a close-up look at the wall. We observe, on the same scale, the difference in magnitude between the overheating obtained with Roe's scheme

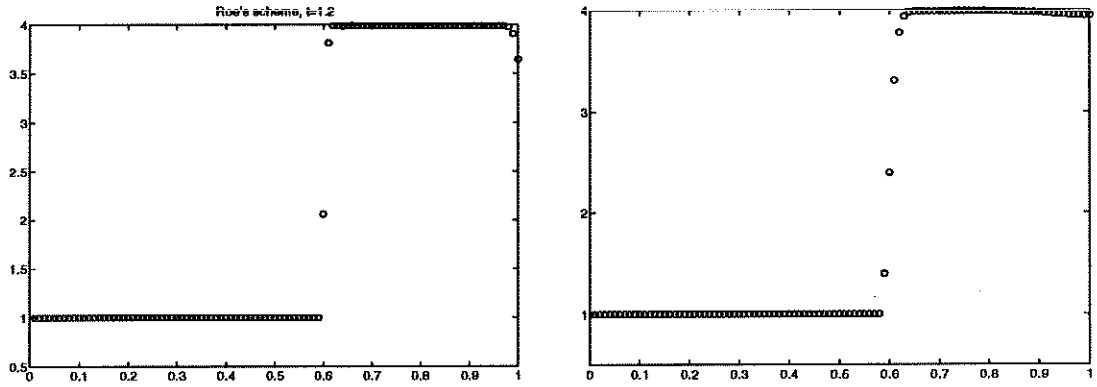

Figure 3: Density profiles: First order schemes.

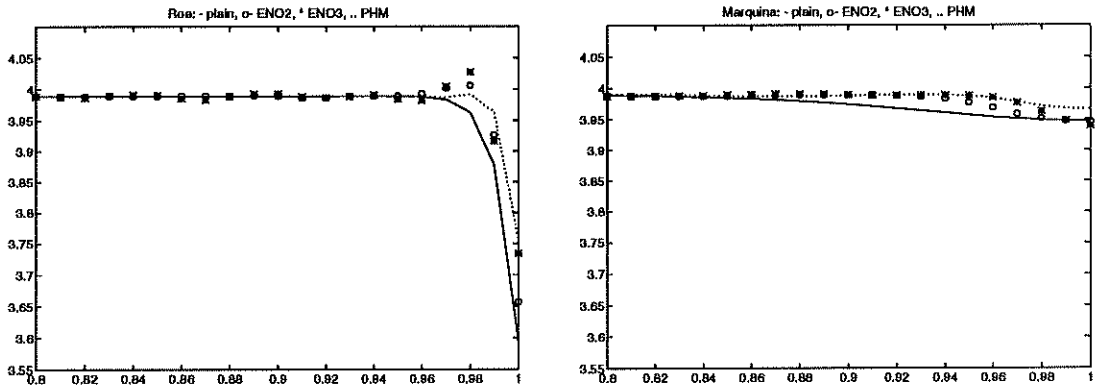

Figure 4: A closer look to the overheating phenomenon.

and its higher order versions and Marquina's scheme and its corresponding higher order extensions. We should remark that the error at the bottom of the spike in the numerical approximation obtained with Marquina's solver (first order) is less than 1% . This should be compared with the 10% error at the bottom of the spike obtained with Roe's scheme (or even with the 100% error obtained with the standard artificial viscosity method [13]).

It is worth noticing that the numerical approximation obtained with Marquina's flux formula and the PHM provides the best resolution.

In the first few steps, Roe's scheme estimates erroneously the shock speed, which is essentially wrong by $O(1)$, this in turn gives $O(1)$ errors for the density. Roe's scheme never recovers from these first steps errors because the error appears in the contact wave but, since the flow velocity is everywhere zero behind the shock wave, no dissipation is added via the contact wave to damp out the

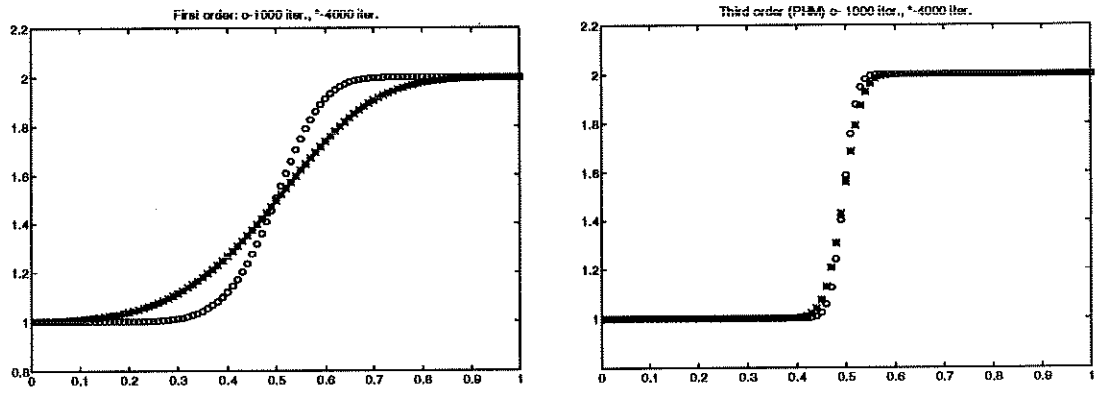

Figure 5: Marquina's scheme. Density profile: o- t=1, *- t=4, $\Delta t/\Delta x = .1$

local error at the wall.

Marquina's scheme introduces an effective coupling between the equations (via the α) that acts as a dissipative mechanism, reducing the length of the spike to computationally acceptable levels.

Based on Noh's observations, we could interpret the behavior of the numerical solution obtained with Marquina's flux formula by saying that there may be an artificial heat conduction mechanism built into Marquina's solver which is responsible for the curbing of the spike.

It is well known (eg. [9]) that flux-splitting schemes cannot exactly resolve stationary discontinuities. Contact discontinuities keep on spreading with the use of any split flux scheme.

As we mentioned before, Marquina's scheme is not a flux-splitting scheme, but it seems clear that it does have a built-in heat conduction mechanism. To test the influence Marquina's flux formula has on stationary discontinuities we consider the Riemann problem with left and right states given by

$$(\rho_l = 1, q_l = 0, p_l = 1) \qquad (\rho_r = 2, q_r = 0, p_r = 1) \tag{11}$$

whose solution is just a stationary (contact) discontinuity. Of course, Roe's scheme resolves perfectly this discontinuity (by design). Marquina's flux formula gives non-zero values when the velocity vanishes and the left and right pressures are equal. The artificial heat conduction mechanism tends to smooth out the density.

The result of Marquina's first order accurate scheme is shown in figure 5. As we can see, the density is smoothed with the number of time steps. However, the smoothing is less severe when we increase the order of the scheme.

This is an undesirable property when solving the Navier-Stokes equations in a boundary layer, thus one should be careful in using the scheme in that situation. However, higher order versions of the scheme might still be suitable.

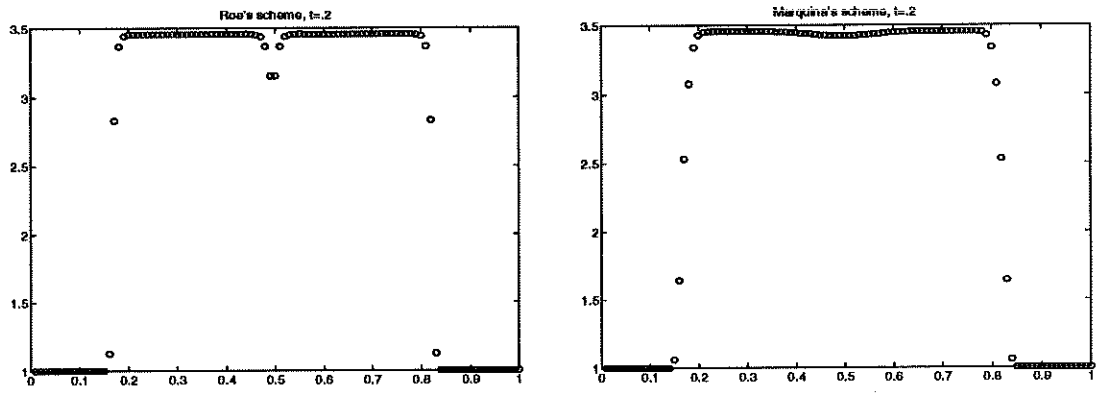

Figure 6: Density profiles: First order schemes.

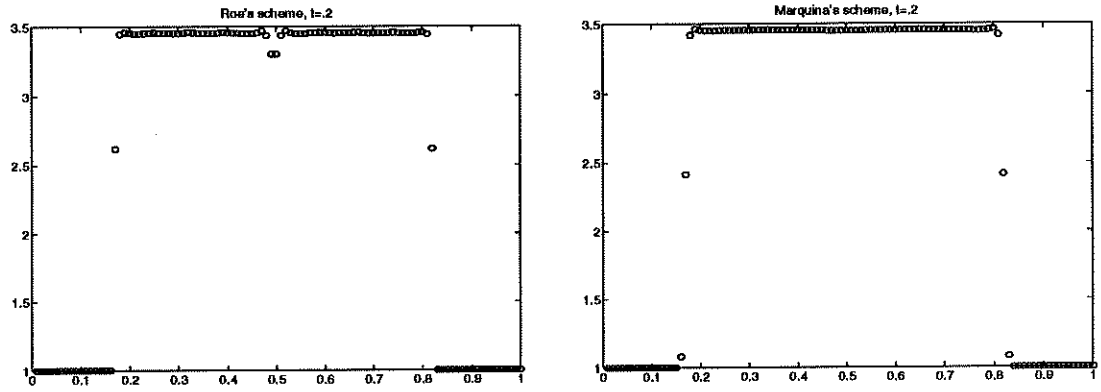

Figure 7: Density profiles: Third order schemes PHM .

Roe's solver not only presents a local spike in the shock reflection case, this behavior can also be observed when an initial discontinuity breaks into two rarefaction waves moving in opposite directions, although in this case the use of any linearization (such as Roe's) might lead to the blow up of the scheme.

Einfeldt et al. show in [4] that certain choices of initial data will inevitably give rise to instabilities with any attempt to substitute linearized solutions because for these data, any linearization will yield a negative density or pressure. They express this fact by saying that certain Riemann problems are not linearizable.

Following [4] we consider the following class of initial data:

$$(\rho(x), q(x), P(x)) = \begin{cases} (\rho_0, q_0, P_0), & \text{if } x < 0.5; \\ (\rho_0, -q_0, P_0), & \text{if } x \geq 0.5. \end{cases} \tag{12}$$

If $q_0 > 0$, two shock waves are formed from the original jump in velocity. They propagate from the center of the interval with constant velocities in opposite directions and the gas remains at rest in between. This is a linearizable problem computationally equivalent to the shock reflection test problem already analyzed.

Numerically, we observe the same type of behavior for both schemes (Roe and Marquina's) as in the previous test, (see figures 6,7). In our numerical experiments we have chosen $(\rho_0, q_0, P_0) = (1, 4, 1)$ and $\Delta t/\Delta x = .1$.

As before, the error at the bottom of the spike in Marquina's solver is less than 1%, while the third order (PHM) scheme has only a .3% error there. In this case, the hyperbolic reconstruction gives the best results, probably due to its more local character. ENO reconstructions (not shown) give slight oscillations of the order of the local truncation error.

If $q < 0$, the problem might not be linearizable, even though it has a solution with positive density and internal energy. The reason for the failure of the linearization is the occurrence of two rarefaction waves in the exact solution to the Riemann problem. Einfeldt et al. consider the particular case where $\rho_0 = 1$,$q_0 = -2$, $e_0 = 3$. This Riemann problem is not linearizable and Roe's scheme blows up after a few steps, (but Roe's scheme with Harten's entropy fix does not, see [4]). Marquina's scheme behaves like the HLLE scheme described by Einfeldt [3, 4] (see figure 8).

Figure 9 displays the numerical approximation obtained with an ENO linear reconstruction. This particular reconstruction is also TVD (see [10] and references therein), a property which is not shared by higher order ENO reconstructions or Marquina's PHM. For this experiment, our third order methods have failed, probably due to the almost vacuum conditions of the solution near $x = .5$.

On the other hand, taking $\rho_0 = 1$, $q_0 = -1$, $e_0 = 5$ as initial data leads to a linearizable problem for which the density exhibits non-smooth behavior similar to the shock reflection problem. As observed, the problem is alleviated by using Marquina's solver. Although the behaviour of the numerical approximations obtained with the higher order extensions of Marquina's scheme is not as good as in the shock collision case, the density profiles are still smoother than those obtained with Roe's scheme (see figures 10 11, and 12).

5 Slowly moving Shocks

Another 'deficiency' of Roe's scheme, and in fact of most Godunov-type schemes, is the generation of numerical errors which occurs behind a nearly stationary shock.

The phenomenon is inherent to nonlinear systems of equations (solutions of scalar conservation laws are perfectly well behaved) and typically shows up as a long wavelength noise in the downstream running wave family that is not

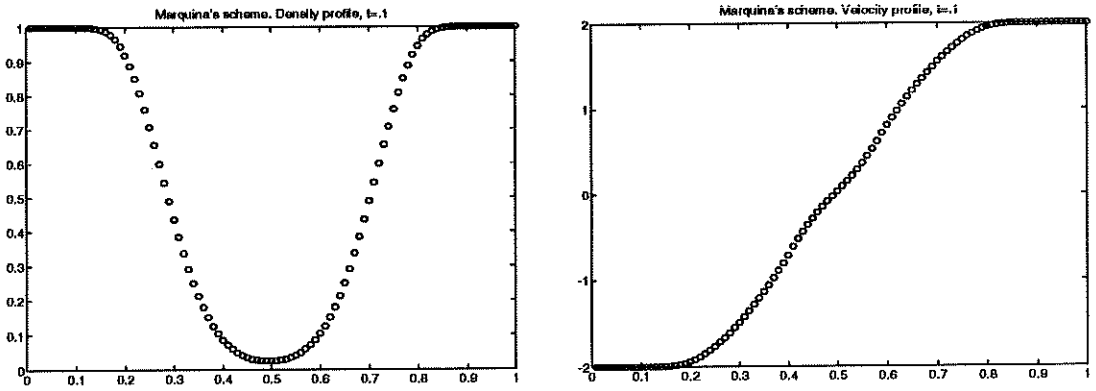

Figure 8: Density profiles: First order scheme

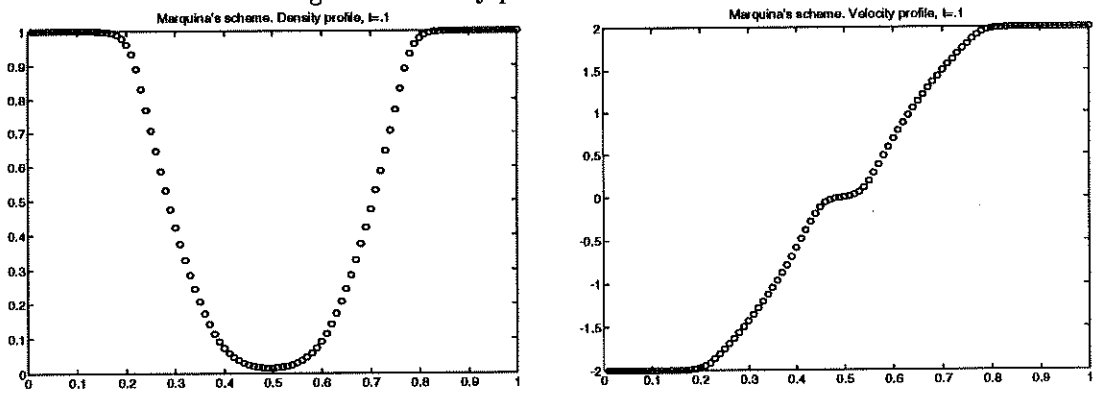

Figure 9: Density profiles: Second order scheme ENO-2

effectively damped by the dissipation of the scheme.

Woodward and Colella [1, 26] were among the first to point out this deficiency for the first order method of Godunov and MUSCL, one of its second order extensions.

In [1] the authors give a heuristic explanation for the noise generation phenomenon and propose a 'cure': the addition of a small amount of artificial dissipation to the underlying scheme.

Roberts [17] performs a deeper analysis of the phenomenon and shows that the cause of the noise generation is linked to the nature of the discrete shock structure produced by each particular scheme. Roberts shows that Osher's scheme [14] does not produce low frequency noise for slowly moving shocks. on the other hand, any scheme that attempts to 'recognize' a shock wave, such as Roe and Godunov's schemes which allow for a perfect representation of a stationary discontinuity, will generate this low frequency perturbation.

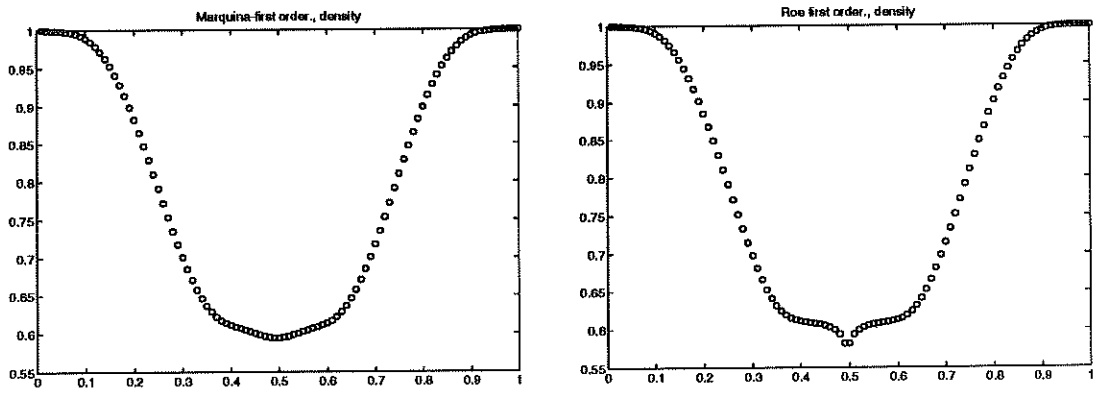

Figure 10: Density profiles: First order schemes

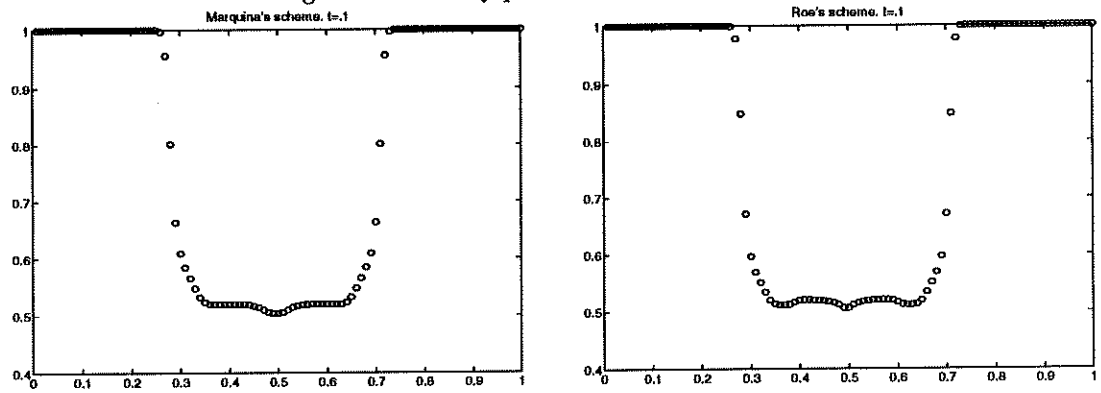

Figure 11: Density profiles: Third order schemes (PHM)

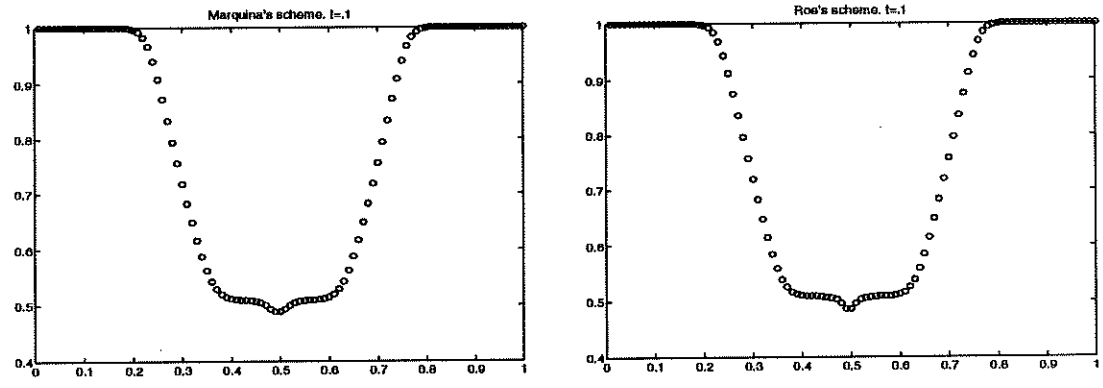

Figure 12: Density profiles: Third order schemes (ENO-3)

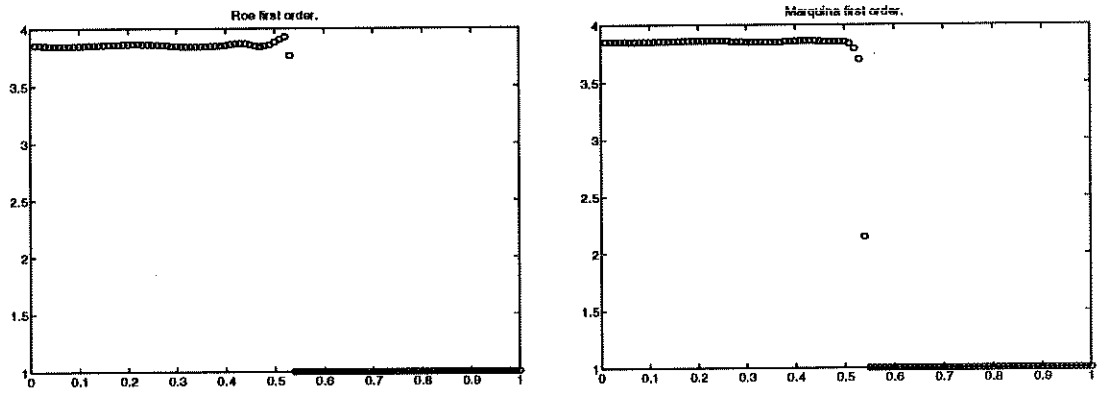

Figure 13: Density profiles: First order schemes.

Roberts further observes that the noise cannot be eliminated by appealing to TVD concepts. In fact, higher order versions of Godunov or Roe's scheme accentuate the problem: the noise is preserved for an even longer distance than in the first order solution.

He concludes by suggesting that numerical flux formulas that recognize the analytical shock jump conditions (such as Godunov or Roe's) might be less appropriate for shock capturing than other formulas that do not explicitly recognize those jumps.

Quirk [15] reports similar low frequency, post-shock oscillations in slowly moving shock waves computed with Einfeld's HLLE scheme [3].

We shall consider the Riemann problem for the Euler equations for an ideal gas with left and right states given by (Quirk [15]):

$$(\rho_l = 1, q_l = -3.44, p_l = 1) \qquad (\rho_r = 3.86, q_r = -0.81, p_r = 10.33) \qquad (13)$$

Our numerical solutions are shown after 4000 iterations, after which the shock has crossed about 42 cells.

We can observe in figures 13 and 14 that the noise generation and transport phenomenon is less acute in Marquina's scheme. It is sensible to think that the heat conduction mechanism is responsible for the additional dissipation that damps out the downstream noise to computationally acceptable levels.

As observed by Roberts [17], the noise is amplified and preserved further downstream in higher order extensions of Roe's scheme. On the other hand, the PHM in Marquina's scheme leads to a higher order method with, essentially, the same properties, with respect to the noise phenomenon, as the first order approximation (see figure 15).

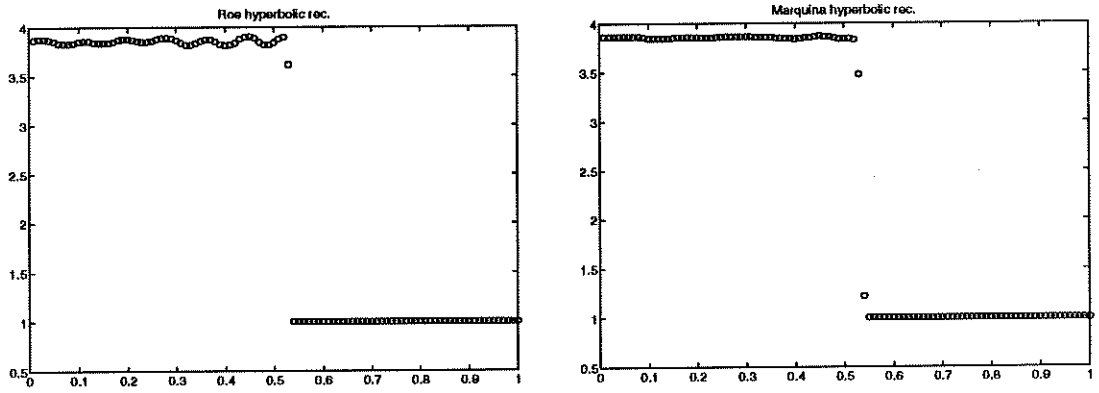

Figure 14: Density profiles: Third order schemes (PHM).

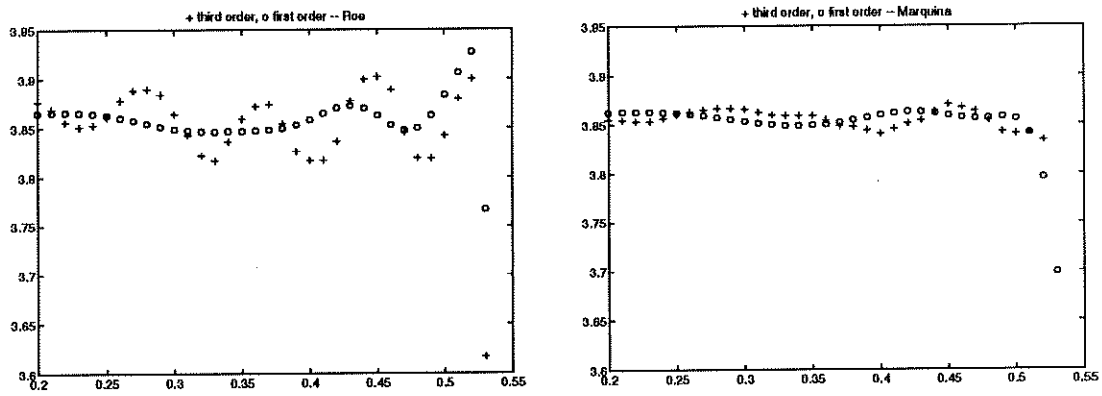

Figure 15: A closer look at the noise in a slowly moving shock

6 A Two Dimensional Test

In this section we consider a two dimensional test problem introduced by Emery [5] almost thirty years ago but that has proven to be a useful test for a large number of methods over the years.

The problem begins with a uniform Mach 3 flow in a tunnel containing a step. The tunnel is 3 units long and 1 unit wide. The step is 0.2 units high and is located 0.6 units from the left-hand end of the tunnel. An inflow boundary condition is applied at the left end of the computational domain and outflow boundary conditions are applied at the right end. Along the walls of the tunnel we apply reflecting boundary conditions.

Initially, the wind tunnel is filled with a gamma-law gas, with γ =1.4, which everywhere has density 1.4, pressure 1.0 and velocity 3. Gas with this density, pressure and velocity is continually fed in from the left-hand boundary.

This test problem receives detailed attention in [26], where the authors analyze the behavior of various shock capturing schemes applied to it. We refer the interested reader to this paper (and references therein) for further details and comparisons.

The density distribution is the hardest to compute due, on one hand, to the Mach stem at the upper wall and the contact discontinuity it generates and, on the other hand, to the corner of the step, which is a singularity of the boundary of the domain and the center of a rarefaction fan, i.e. a singular point of the flow.

Woodward and Colella [26] realize that numerical errors generated in the neighborhood of this singular point can seriously affect the global flow. As pointed out in [26], when an approximate Riemann solver is used, the entropy tends to grow near the corner and along the sonic line starting at the corner. If nothing is done, a numerical boundary layer in density, of about one to two zones, builds up and the magnitude of the two components of the velocity decreases along the top of the step, hence changing the quality of the flow.

In an attempt to minimize numerical errors generated at the corner of the step, Woodward and Colella propose an additional boundary condition to be applied near the corner of the step, in order to maintain a steady flow around this singular point. Our experimentation confirms Woodward and Colella's remarks. It is necessary to correct the entropy near the corner, but we have found that to maintain a steady flow it is also necessary to update the enthalpy. A detailed treatment of the corner correction is given in the appendix.

Our numerical tests are run on an equally spaced grid with $h_x = h_y$ =1/40. and we show numerical approximations to the density profile at time t =4, when the flow has a rich and interesting structure. The extension to two dimensions is done by the usual operator splitting technique.

In Figure 16 we display the density profiles obtained with Marquina's scheme. Figure 17 shows the results of similar runs obtained with Roe's scheme.

The Mach stem in Roe's approximation appears severely distorted by a "dou-

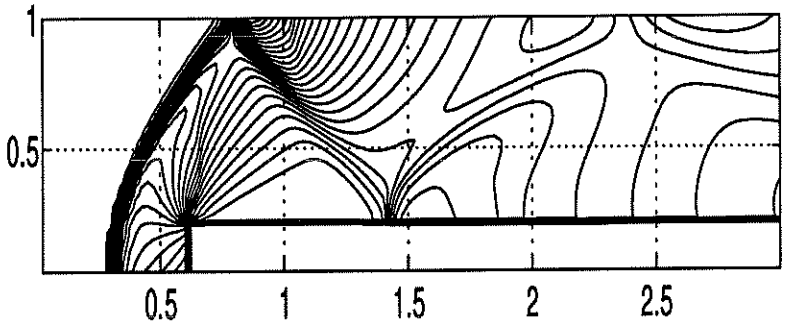

(a): First Order, no reconstr., 30 level curv. between min=1.17, max =7.19,

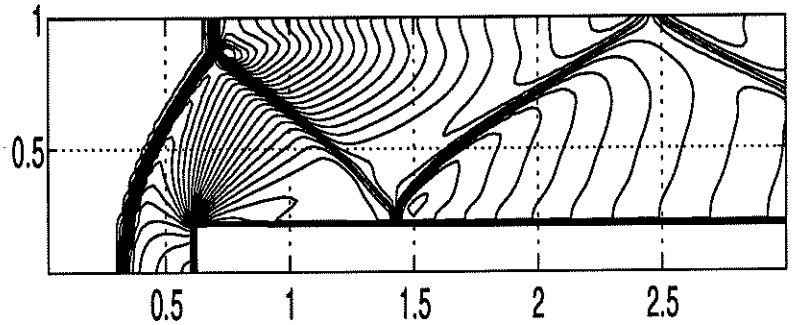

(b): MUSCL Reconstr., 30 level curv. between min=0.73 and max=6.37

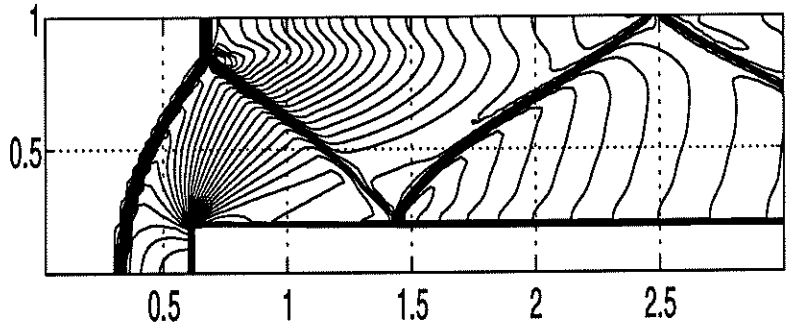

(c): Hyperbolic Recons., 30 level curv. between min=0.64 and max=6.4 4 ,

Figure 16:

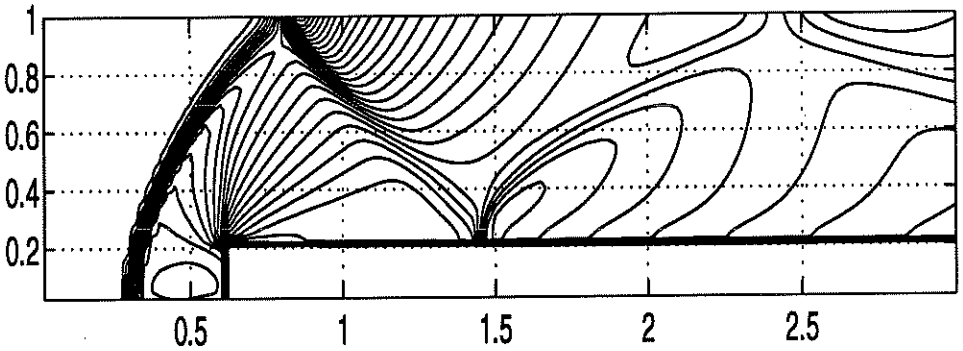

(a): Roe First Order, no reconstr., 30 level curv. between min=0.81, max=7.85,

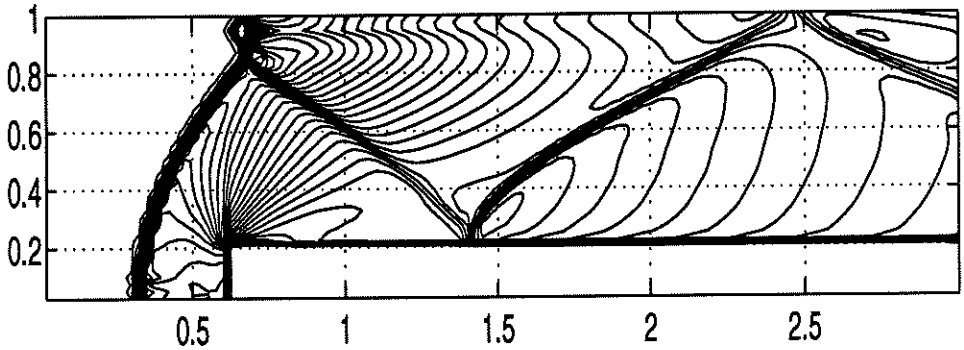

(b): Roe with MUSCL Reconstr., 30 level curv. between min=0.51 and max=6.55

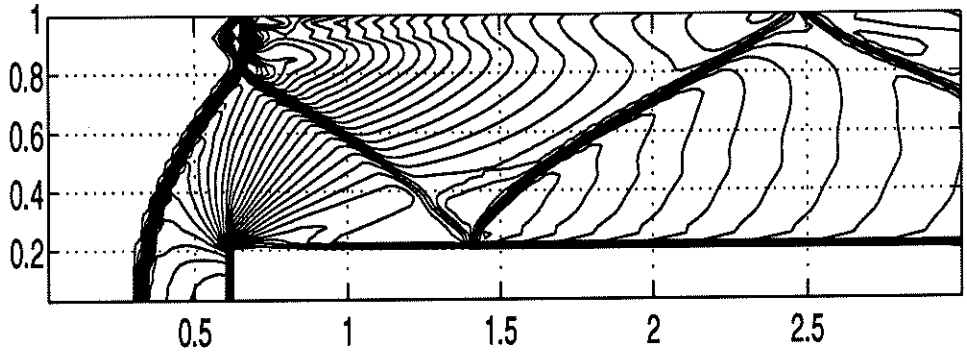

(c): Roe with Hyperbolic Recons., 30 level curv. between min=0.40 and max=6.43 ,

Figure 17:

ble kink". This phenomenon is not dissimilar to the "carbuncle", a recognized deficiency of Roe's scheme observed in steady-state blunt body calculations [16].

By time t =4, nearly all shocks in this problem are moving very slowly. In particular, the bow shock is nearly aligned with the grid near the bottom wall, leading to a scenario like the one described in section 5. The post-shock oscillations are more visible when using Van Leer's piecewise linear reconstruction [22].

To eliminate the 'carbuncle' produced in Roe's scheme one has to artificially add dissipation to the scheme. Peery and Imlay [16] do so by an appropriate smoothing of the eigenvalues o the Roe matrix. Quirk [15] reports that applying Harten's entropy fix to the contact and shear waves also fixes the problem. Both alternatives become a convenient way to introduce a small (but sufficient) amount of artificial dissipation into the scheme.

As in our one-dimensional tests, Marquina's scheme seems to introduce the right amount of dissipation to eliminate the undesired pathologies, while keeping, at the same time, sharp shock structures.

7 Conclusions

We extend to systems a numerical flux formula proposed by Shu and Osher [20] for scalar equations. The extension is made in each local characteristic field and does not need of a mean state (such as Roe's average or the arithmetic mean) which turns out to be useful in certain situations, where even an approximate solution to the Riemann problem is difficult to compute.

Marquina's flux formula seems to introduce a dissipative mechanism into the numerical scheme which, in turn, produces numerical approximations with a smoother behavior than those obtained with Roe's scheme, while keeping, essentially, the sharp shock resolution of this method. In particular, the overheating phenomenon observed near the piston wall in shock reflection experiments is greatly reduced, as well as the long wavelength noise behind slowly moving shock waves.

Preliminary experimentation in two dimensions seems to confirm that the dissipation of the scheme is sufficient to eliminate undesired pathologies like the carbuncle phenomenon.

Acknowledgements The authors thank J.M. Ibañez, J.M. Marti and J.A. Font for many useful dicussions and comments. We also thank S. Osher and A. Harten for their valuable remarks. We specially thank P.L. Roe and the referees of this paper for their remarks and for providing several useful references.

References

[1] P. Colella and P.R. Woodward, *The Piecewise Parabolic Method for Gas Dynamics,* J. Comput. Phys., v. **54**, pp. 174, (1984)

[2] R. Courant and K.O. Friedrichs,*Supersonic Flow and Shock Waves,* Springer-Verlag, New York, (1976).

[3] B. Einfeldt, *On Godunov type methods for Gas Dynamics,* SINUM v. **25**, (1988) pp. 294-318.

[4] B. Einfeldt,, C.D. Munz, P.L. Roe, B. Sjögreen *On Godunov type methods near low densities,* J. Comput. Phys., v. **92**, (1991) pp. 273-295.

[5] A.F. Emery, *An Evaluation of Several Differencing Methods for Inviscid Fluid Flow Problems,* J. Comp. Phys., **2**, p. 306-331, (1968).

[6] P. Glaister, *An Approximate Linearized Riemann Solver for the Euler Equations for Real Gases,* J. Comp. Phys., **74**, p. 382-408, (1988).

[7] A. Harten, J.M. Hyman *Self Adjusting Grid Methods for One-Dimensional Hyperbolic Conservation Laws,* J. Comput. Phys., v. **50**, (1983) pp. 235-269.

[8] A. Harten, J.M. Hyman and P.D. Lax, *On Finite-Difference Approximations and Entropy Conditions for Shocks,* Comm. Pure Appl. Math., **29**, 297 (1976).

[9] A. Harten, P.D. Lax and B. van Leer, *On Upstream differencing and Godunov type Schemes for Hyperbolic Conservation Laws,* SIAM Review, **25**, pp. 35-61 (1983).

[10] A. Harten, B. Engquist, S. Osher and S. Chakravarthy, *Uniformly High Order Accurate Essentially Non-oscillatory Schemes III,* J. Comput. Phys., v. **71** No. 2, (1987), pp. 231-303.

[11] A. Marquina, *Local Piecewise Hyperbolic Reconstructions for Nonlinear Scalar Conservation Laws,* UCLA CAM Report No. 25-(1989), SIAM J. Scientific Comp., v. **15**, (1994) pp. 892-915.

[12] R. Menikoff, *Errors when Shock waves interact due to numerical shock width,* SIAM J. Scientific Comp., v. **15**, (1994) pp. 1242-1277.

[13] W.F. Noh, *Errors for the Calculations of Strong Shocks using an artificial viscosity and an artificial heat flux,* J. Comput. Phys., v. **72**, (1987) pp. 78-120.

[14] S. Osher, F. Solomon, *Upwind difference schemes for hyperbolic systems of Conservation Laws,* Math. Comput., v. **38**, (1982) pp. 339-374.

[15] J. Quirk, *A contribution to the great Riemann Solver debate,* ICASE Report 92-64 (1992).

[16] K.M. Peery and S.T. Imlay, *Blunt Body Flow Simulations,* AAIA paper 88-2904

[17] T. W. Roberts, *The behavior of flux-difference splitting schemes near slowly moving shock waves,* J. Comput. Phys. v **90** (1990) pp 141-160.

[18] P. L. Roe, *Sonic Flux Formulae,* SIAM J. Scientific Comp., v. **13**, No.2, (1992), pp. 611-630.

[19] R. Sanders and A. Weiser, *High Resolution Staggered Mesh Approach for non-linear Hyperbolic Systems of Conservation Laws,* J. Comput. Physics, **101**, (1992), pp. 314-329.

[20] C. W. Shu and S. J. Osher, *Efficient Implementation of Essentially Non-Oscillatory Shock Capturing Schemes II,* J. Comput. Phys., v. **83**, (1989) pp. 32-78.

[21] J. Steger and R.F. Warming *Flux Vector Splitting of the Inviscid Gasdynamics Equations with Application to Finite Difference Methods,* J. Comput. Phys., v. **40**, (1981) pp. 263-293.

[22] B. Van Leer, *Towards the ultimate conservative difference scheme V. A second order sequel to Godunov's method,* J. Comput. Phys.,**32**,(1979), p.101-136.

[23] B. Van Leer, *On the relation between the Upwind-Differencing schemes of Godunov, Engquist-Osher and Roe,* SIAM J. Sci. Stat. Comput.,**5**,(1984), p.1-20.

[24] B. Van Leer, *Flux-vector splitting for the Euler equations,* presented aat the 8th international Conference on Numerical Methods for Engineering, Aachen, June 1982.

[25] P.R. Woodward and P. Colella, High Resolution Difference Scheme for Compressible Gas Dynamics, Seventh Interntl. Conf. on Num. Methods in Fluid Dynamics, Lecture Notes in Physics, Vol. 141, pp. 434-441, (1981).

[26] P.R. Woodward and P. Colella, *The Numerical Simulation of Two-Dimensional Fluid Flow with Strong Shocks,* J. Comput. Phys., v. **54**, (1984) pp. 115-173

Appendix: Discussion of the Corner Treatment

In order to go further into the discussion of the influence of the corner treatment in Emery's test, we shall explain in detail the process introduced in [26] and outlined in [19] (where we have observed various typographycal errors).

We shall perform two successive corrections on certain cells, which we call "b", above the step, using the values of the variables at the cell located just to the left and below the corner, we call this cell "a" (as in [19]). The "b" cells are the first four cells of the first row above the step starting just to the right of the corner, and the first two cells of the second row above, also starting from the right.

The corrections should be as follows:

- *Entropy Correction* In each "b" cell, we reset the density in order for the adiabatic constant in cell "b", to be the same as in cell "a".

$$\rho_b = \rho_a \left(\frac{P_b}{P_a}\right)^{\frac{1}{\gamma}} \tag{14}$$

- *Enthalpy Correction* Using the reset density value, we correct the enthalpy in "b" cells, by changing the magnitudes of the velocities (not their directions!) as follows:

  There is always a non negative constant α such that

$$H_a = H_b^{\alpha} \tag{15}$$

  where H_a is the enthalpy in cell "a", and

$$H_b^{\alpha} = \frac{c_b^2}{(\gamma - 1)} + \frac{1}{2}\alpha q_b^2 \tag{16}$$

  with q_b^2 being the sum of the squares of the original components of the velocity in cell "b", and c_b the sound velocity computed from the new value of the density also in cell "b". The equation (15) is just *Bernouilli's law* for steady flow, (see [2]), and it always has a nonnegative solution for α, because the value of the density in "b" cells is never larger than the value in cell "a".

  Indeed, if $A = \frac{P_a}{\rho_a^{\gamma}}$ is the adiabatic constant in cell "a", then, because of the entropy correction performed before, we have that $A = \frac{P_b}{\rho_b^{\gamma}}$,and, therefore, α is nonnegative and defined by

$$\alpha = \frac{\frac{1}{2}q_a^2 + \frac{\gamma}{\gamma-1}A\left(\rho_a^{\gamma-1} - \rho_b^{\gamma-1}\right)}{\frac{1}{2}q_b^2} \tag{17}$$

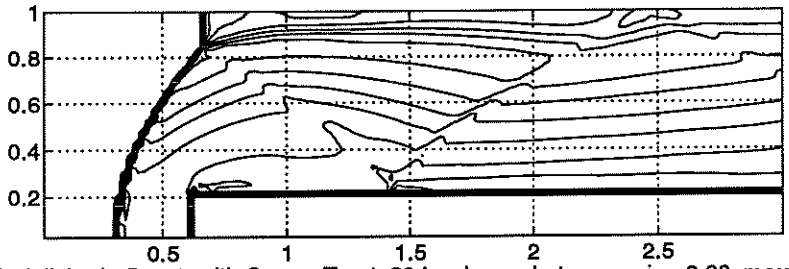

(a): Adiabatic Const. with Corner Treat. 30 level curv. between min= 0.62, max=1.13,

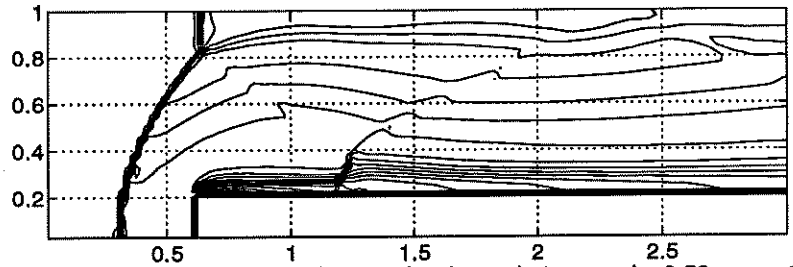

(b): Adiab. Const. No Corner Treat. 30 level curv. between min=0.56, max=1.56,

Figure 18:

We then reset the vector $\mathbf{u}$ in each "b" cell to

$$\left(\rho_b, \sqrt{\alpha}(q_b)_x, \sqrt{\alpha}(q_b)_y, \frac{1}{\gamma-1}P_b + \frac{1}{2}\rho_b \alpha q_b^2\right) \tag{18}$$

If these two successive corrections are not applied the adiabatic constant, (and a *fortiori* the entropy), is violated along the streamlines just above the step.

In Figure 18 we display two contour plots of the adiabatic constant at $t = 4..$ They correspond to numerical approximations obtained with Marquina's scheme and the PHM as the reconstruction procedure. 18 (a) corresponds to the application of the corner treatment and 18 (b) without this treatment.

We have observed that, when no treatment is applied, the value of the enthalpy above and near the corner is slightly smaller than the value at the left of the corner. Thus the fluid there is almost steady, however, the entropy is clearly violated and we get analogous pictures to the ones presented in [25].

The reason we need to apply the two corrections is that if only the entropy is corrected, then, the flow near the corner becomes far from steady, and the enthalpy is abruptly going down at the right of the sonic line, (see Figure 19).

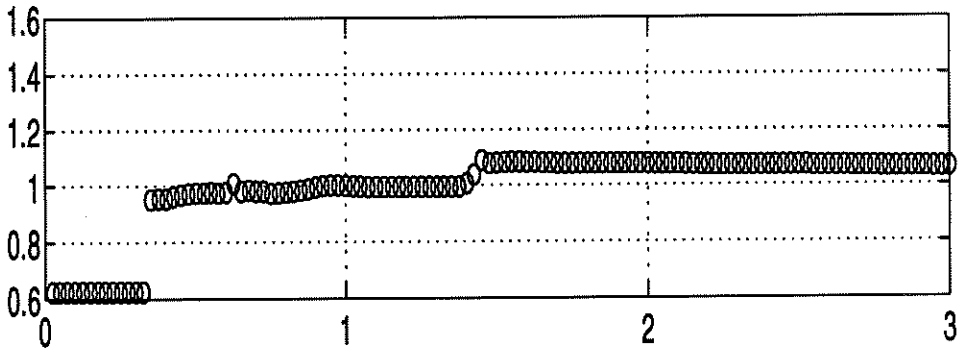

Adiab. Const., Section y=0.2 with Corner Treatment

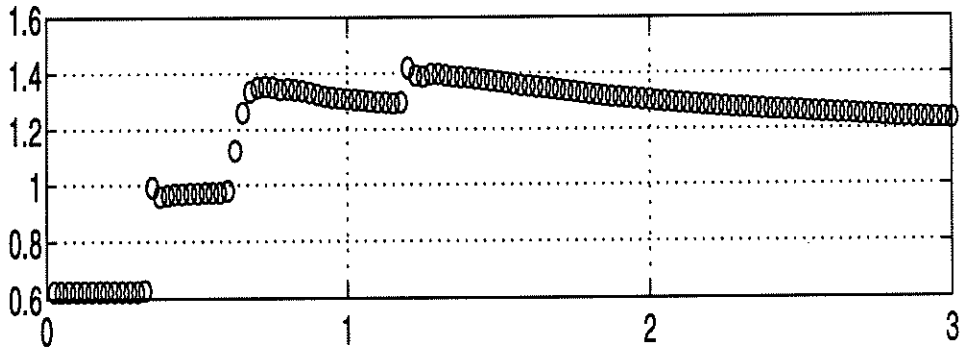

Adiab. Const., Section y=0.2 with No Corner Treatment

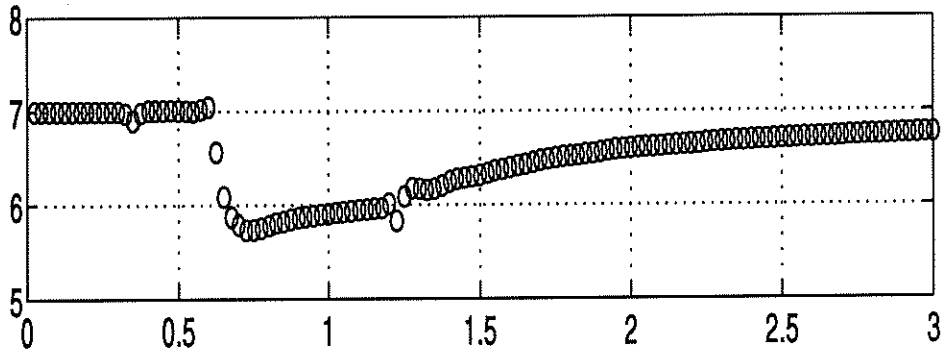

Enthalpy Section y=0.2 with Entropy Correction and No Enthalpy Update

Figure 19:

The section $y = 0.2$ of the adiabatic constant is shown in Figure 19 for both cases. We observe a strong entropy violation at $x = .6$, the abscissa of the corner. This section can be considered nearly a streamline of the flow.

We consider this a fair numerical test in order to evaluate the reliability of the numerical approximation. We have computed numerical approximations to the solution of this problem using our solver with a finer grid, (e.g., 240x80), and the profiles obtained are consistent with the features presented with the 120x40 grid and the order of accuracy used.